Author Manuscript

Author Manuscript

Author Manuscript

Author Manuscript

HHS Public Access

Author manuscript

J Magn Reson Imaging. Author manuscript; available in PMC 2016 June 01.

Published in final edited form as:

J Magn Reson Imaging. 2015 June ; 41(6): 1689–1694. doi:10.1002/jmri.24696.

Computer-Automated Focus Lateralization of Temporal Lobe Epilepsy using fMRI

Sharon Chiang, B.A.[1,6], **Harvey S. Levin, Ph.D.**[2,3], and **Zulfi Haneef, M.D., F.R.C.P.**[4,5,6,*]

[1]Department of Statistics, Rice University, Houston, Texas

[2]Department of Physical Medicine, Baylor College of Medicine, Houston, Texas

[3]Michael E. DeBakey VA Medical Center, Houston, Texas

[4]Department of Neurology, Baylor College of Medicine, Houston, Texas

[5]Neurology Care Line, VA Medical Center, Houston, Texas

Abstract

Purpose—To compare the performance of computer-automated diagnosis using fMRI interictal graph theory (CADFIG) to that achieved in standard clinical practice with MRI, for lateralizing the affected hemisphere in temporal lobe epilepsy (TLE).

Materials and Methods—Interictal resting state fMRI and high-resolution MRI were performed on 14 left and 10 right TLE patients. Functional topology measures were calculated from fMRI using graph theory, and used to lateralize the epileptogenic hemisphere using quadratic discriminant analysis. Leave-one-out cross-validation prediction accuracy of CADFIG was compared to performance based on expert manual analysis (MA) of MRI, using video EEG as the "gold standard" for focus lateralization.

Results—CADFIG correctly lateralized 95.8% (23/24) of cases, compared to 66.7% (16/24) with expert MA of MRI. Combining MA with CADFIG allowed all cases (24/24) to be correctly lateralized. CADFIG correctly identified the affected hemisphere for all patients (8/8) where MRI failed to lateralize.

Conclusion—CADFIG based on fMRI lateralized the affected hemisphere in TLE with superior performance compared to expert MA of MRI. These results demonstrate that functional patterns in fMRI can be used with automated machine learning for diagnostic lateralization in TLE. Addition of fMRI-based tests to existing protocols for identifying the affected hemisphere in pre-surgical assessment can improve diagnostic accuracy and surgical outcome in TLE.

Keywords

Functional magnetic resonance imaging; Graph theory; Temporal lobe epilepsy; Lateralization; Functional connectivity; Automated pattern recognition

[*]Address all correspondence to: Zulfi Haneef, M.D., F.R.C.P. Assistant Professor of Neurology, Peter Kellaway Section of Neurophysiology, Department of Neurology, Baylor College of Medicine, One Baylor Plaza, MS: NB302, Houston, TX 77030, Telephone Number: +1-832-355-4044, Facsimile Number: +1-713-798-7561, zulfi.haneef@bcm.edu.

[6]Both authors contributed equally to this work.

Author Manuscript Author Manuscript Author Manuscript Author Manuscript

INTRODUCTION

Temporal lobe epilepsy (TLE) is the most common pharmacoresistant and surgically remediable epilepsy in adults. However, surgery is denied in 30%, primarily due to unclear localizing evidence from pre-surgical testing (1). In standard pre-surgical evaluation, high-resolution MRI plays a central role. Discordance or non-concordance of MRI with video-electroencephalography (VEEG) hampers the pre-surgical workup, with 30-40% of patients with EEG evidence of TLE showing normal or non-lateralizing MRI scans (1,2).

Accurate lateralization reported with non-invasive tests is 70-85% (MRI), 60-90% (positron emission tomography, PET), 50-90% (magnetoencephalogram, MEG), and >90% (single-photon emission computed tomography, SPECT) (2). MRI is considered the best non-invasive test to define the epileptogenic lesion (3). However, functional imaging provides complementary information to structural imaging such as MRI (2), and may improve TLE lateralization.

Recent neuroimaging advances have stimulated interest in using pattern extraction based on machine learning to perform brain image classification. Machine learning techniques have demonstrated potential for improving epileptogenic lateralization using various structural and metabolic imaging tests, including MRI (85-95%) and SPECT (95%) (4,5). Functional connectivity MRI (fcMRI) has recently gained popularity in TLE connectivity research due to the characterization of TLE as a “network disease” (2). Graph theory provides an effective model for quantifying connectome patterns in resting-state fMRI (rs-fMRI) (6). However, to our knowledge, fMRI graph theory has not been used for lateralizing TLE on a prospective subject-level basis using machine learning.

Here, we employed a graph theory model of interictal rs-fMRI data to estimate measures of brain topology. We showed that lateralized differences in fMRI graph theory measures can be used to prospectively predict the epileptogenic hemisphere in TLE with high sensitivity, and propose one such computer-automated diagnostic approach using fMRI interictal graph theory (CADFIG). Application of fMRI-based tests such as CADFIG for pre-surgical epilepsy assessment may aid TLE lateralization. The objectives of this study were to (1) evaluate the sensitivity of CADFIG for TLE lateralization, (2) compare performance of CADFIG to MRI, which is clinically proven in lateralizing TLE, and (3) compare the relative discriminatory capabilities of various fMRI graph theory measures in lateralizing TLE.

MATERIALS AND METHODS

Patients

Twenty-four TLE patients were recruited from our institution’s comprehensive epilepsy center and underwent inpatient VEEG and a high-resolution MR imaging session. Patients with (1) bilateral TLE or (2) significant cognitive impairment or major neurological/psychiatric co-morbidities were excluded. The study protocol was approved by our institutional review board and informed consent obtained from study participants.

Author Manuscript Author Manuscript Author Manuscript Author Manuscript

Video-EEG Monitoring

Inpatient VEEG was used as the "gold standard" for epileptogenic lateralization, following previous studies (7). Including only patients with unequivocal VEEG lateralization, 14 patients had left TLE and 10 had right TLE (Supplementary Table 1).

Image Acquisition

MR imaging was performed on a 3.0 Tesla scanner (Ingenia, Philips Healthcare, Best, Netherlands). 3D IR-TFE imaging parameters were: 220 phase encoding steps; TR/TE=8ms/4.0ms; flip angle=8°; time between successive TFE shots=3000ms; FOV=240×220×170mm^3; acquired voxel size=1×1×1mm^3. A parallel imaging acceleration factor of two was applied along the slice direction. A volumetric T_2-prepared 3D-FLAIR with variable refocusing angle modulation was used to obtain CSF-attenuated, T_2-weighted images: TR/TI=4800ms/1650ms; T_2-preparation time=125ms (four refocusing pulses); turbo-spin echo readout duration=640 ms (inter-echo spacing=3.2ms); acquired voxel size=1.1×1.1×1.1mm^3; scan time=06:57min. A refocusing pulse modulation was used to attain an effective TE of 142 ms (equivalent TE of 320 ms). A parallel imaging acceleration factor of two was applied along each phase encoding direction (phase/slice). Rs-fMRI was acquired axially for 10 minutes with: TR=6000ms, TE=30ms, FOV=228mm, matrix=100×100, slice thickness=2.25mm, 67 slices, 100 volumes. Patients were instructed to lie still with eyes closed, and asked not to think about anything in particular during the functional sequences. The imaging technician ensured that the subjects did not fall asleep during imaging. No auditory stimulus was present other than acoustic noise from imaging.

BOLD fMRI Image Pre-processing

Data pre-processing were performed using FSL (fMRIB Software Library) version 5.0.2 (Oxford, UK, www.fmrib.ox.ac.uk/fsl). The first 12 seconds were discarded to attain magnetization equilibrium. Common pre-processing steps for rs-fMRI were applied (8). These included non-brain tissue elimination; slice-timing correction; spatial smoothing using a Gaussian kernel (5-mm FWHM); linear co-registration to the T_1-weighted image; temporal bandpass filtering ($0.01<f<0.08$ Hz) and removal of sources of spurious variance using linear regression: six motion parameters and temporal derivatives, ventricular and white matter signal. Whole-brain signal regression was not performed, in order to increase test-retest reliability in graph theory analyses (9). Motion scrubbing was also performed (10). Residuals were normalized prior to analysis.

Brain Parcellation and Graph Construction

After linear registration to the MNI standard, functional images were parcellated into ninety anatomical regions using an automated anatomical labeling atlas (11). fMRI residual time series were averaged across all voxels in each region. Functional connectivity was estimated by the Pearson correlation coefficient between residual time series.

Negative correlations were set to zero to improve the reliability of graph theory metrics (12). Unweighted graphs were constructed by thresholding the correlation matrix across the

Author Manuscript Author Manuscript Author Manuscript Author Manuscript

biologically plausible range of connection densities (6), yielding a range of potential undirected graphs of the brain's functional network.

FMRI Features, Feature Selection, and Discriminant Analysis

Expert manual analysis (MA) of T_1-weighted, T_2-weighted, and FLAIR sequences was performed by neuroradiologists experienced in the interpretation of epilepsy neuroimaging. Based on MA reports, baseline measures of lateralization sensitivity encountered in standard clinical practice were obtained by calculating the ratio of correctly lateralized to total cases for left, right, and overall TLE groups.

Several functional topology measures can be calculated for brain networks; however, the relevance of many in TLE is unclear. We focused on graph measures which reflect (1) basic small-world properties of network topology: clustering coefficient (γ), characteristic path length (λ), small-world index (σ), and global efficiency (GE) (6,13); (2) first and second mathematical sample moments of the connectivity matrix: connectivity strength (CS) and connectivity diversity (CD); and (3) regional measures implicated in TLE: betweenness centrality (BC), local efficiency (LE), and regional clustering coefficient (CC) of the left and right hippocampi (13) (Appendix A). Because of the large number and correlation between fMRI features, feature dimension reduction was necessary. All subsets feature selection was performed using quadratic discriminant analysis (QDA) with all subsets of extracted fMRI features compared with respect to leave-one-out cross-validation (LOO-CV) error. QDA was used to classify epileptogenic focus laterality using the selected set of fMRI features based on maximum *a posteriori* assignment. For validation, LOO-CV error was used to assess final classification performance. Details on QDA and LOO-CV are in Appendix B.

Performance Assessment

Sensitivities of MA and CADFIG were assessed by calculating the ratio of the number of correctly classified to total patients for left, right, and overall TLE groups. The sensitivity of a combined approach defined by using either test (i.e., MA, or CADFIG when MA was not concordant with VEEG) was also evaluated. The area under the ROC curve (AUC) was assessed as a general performance measures. McNemar's test was used to investigate improved sensitivity using CADFIG compared to MA alone, as well as a combined approach of CADFIG+MA compared to MA alone. Agreement between MA and CADFIG was evaluated using Cohen's weighted kappa (κ) statistic.

FMRI Feature Ranking

Univariate discriminatory ability of fMRI features was assessed based on the Fisher separability criterion (FSC). To assess the relative contribution of fMRI features to the multivariate discriminatory function, backward stepwise variable importance (BSVI) was used. All statistical analyses were performed using R version 3.0.1 (R Foundation, Vienna, Austria). Details on FSC and BSVI are in Appendix C.

Author Manuscript Author Manuscript Author Manuscript Author Manuscript

RESULTS

CADFIG

CADFIG correctly predicted focus laterality in a significantly greater proportion of TLE subjects (23/24 or 95.8%) than MA (16/24 or 66.7%) (*p*-value 0.045), with a 42.9% increase in sensitivity for right TLE (10/10 or 100% for CADFIG, versus 7/10 or 70.0% for MA) and a 44.4% increase in sensitivity for left TLE (13/14 or 92.9% for CADFIG, versus 9/14 or 64.3% for MA) (Figure 1). This equated to an 11.5 times greater odds of correctly lateralizing the epileptogenic focus using CADFIG. For both left and right TLE, the AUC for CADFIG was 0.96 (95% confidence interval, 0.87-1.00) (Figure 2).

Figure 3a shows coronal FLAIR demonstrating left hippocampal hyperintensity and atrophy from a patient for whom both MA and CADFIG accurately identified the epileptogenic hemisphere (Subject 1, Supplementary Table 1). Much greater agreement was identified between CADFIG and VEEG (κ=0.92) than between MA and VEEG (κ=0.34). Cases lateralized by MA had good agreement of focus laterality between CADFIG and MA (κ=0.88).

Combined Approach of fMRI and MA

CADFIG correctly identified focus laterality in all cases where MA was non-lateralizing or discordant (8/8 or 100%). Figure 3b shows coronal FLAIR in a patient with non-lateralized MRI, but accurately lateralized CADFIG (Subject 13, Supplementary Table 1). A combined CADFIG+MA approach accurately identified focus laterality in all cases (24/24 or 100%). This provided a significant improvement over the classification accuracy of MA alone (16/24 or 66.7%) (*p*-value 0.013).

fMRI Feature Ranking

Figure 4 provides multivariate visualization of the fMRI graph theory measures identified in the optimal feature subset (CD, GE, BC of left and right hippocampi). At a univariate level, left hippocampal BC had the highest discriminative ability (Table 1). Considered in the context of other variables, most features retained relative ranks of importance. However, left hippocampal BC became less essential to the discriminatory function when GE, CD, and right hippocampal BC were taken into account. GE had a relatively greater contribution to the discriminatory function ($BSVI_{GE}$=0.333) than left hippocampal BC ($BSVI_{BC(L)}$=0.292). Left hippocampal BC was much more relatively discriminatory ($FSC_{BC(L)}$=1.468; $BSVI_{BC(L)}$=0.292) than right hippocampal BC ($FSC_{BC(R)}$=0.089; $BSVI_{BC(R)}$=0.125) (Table 1).

DISCUSSION

We investigated whether fMRI-based measures of functional network topology reliably discriminate left and right TLE. We propose one such approach, CADFIG, and demonstrate its superior performance over MA in lateralizing TLE, with all cases of focus laterality correctly predicted when CADFIG was used in conjunction with MA. Graph theory measures of fMRI data have not been used previously for computer-automated TLE

Author Manuscript Author Manuscript Author Manuscript Author Manuscript

lateralization to our knowledge. High sensitivity of CADFIG at an individual subject level illustrates the potential use of fMRI in the pre-surgical TLE workup. Additionally, we propose a combined multimodal approach for seizure lateralization based on fMRI and MRI manual analysis, which attains higher sensitivity than either modality alone. This illustrates the utility of combining structural and functional MR imaging in TLE.

We show that abnormalities not visible on MRI may be detectable using fMRI in TLE. Our novel finding that features extracted from fMRI are able to discriminate the affected hemisphere with high sensitivity corresponds with published data showing that left and right TLE differ with respect to the functional connectome (14).

Left hippocampal BC had the highest univariate discriminatory value for lateralizing TLE. The contralateral hippocampus generally had greater BC than the ipsilateral hippocampus in both left and right TLE (Figure 4). Increased contralateral hippocampal BC may suggest a shift in hub importance from the ipsilateral to contralateral hippocampus. This is congruent with prior reports of increased contralateral hippocampal functional connectivity co-occurring with reduced ipsilateral hippocampal connectivity (15) and correlation of BC with the clinically resected epileptogenic zone (16).

Discriminatory power was much lower for right than left hippocampal BC. Although high left hippocampal BC most likely indicated a right-sided epileptogenic focus and low left hippocampal BC most likely indicated a left-sided epileptogenic focus, such a clear difference did not exist for right hippocampal BC. One possible reason includes higher plasticity of the left hippocampus for assuming lost functionality in TLE. This is supported by increased activation of the contralateral hippocampus identified in right, but not left, TLE (17).

Although CD and GE did not individually discriminate well between left and right TLE, a clear decision boundary was identified when considered together (Figure 4, pairwise CD/GE plot). When considered simultaneously, discriminatory power of CD and GE exceeded that of left hippocampal BC (Table 1). The non-linear separation boundary, however, masks the high discriminatory ability of CD and GE, demonstrating the need for multivariate techniques when discriminating left from right TLE.

The high discriminatory power of GE and CD corresponds with decreased white matter global efficiency in left TLE (18) and a 17 times more abnormal connectivity network in right TLE (19). CD also differs between schizophrenia and controls (20), and may suggest different propensities toward psychosis of epilepsy between left and right TLE. In our study, although CD was on average greater in right than left TLE for patients with low GE, the opposite was true for patients with high GE. This is apparent from the biconcave discrimination boundary in the pairwise scatterplot of CD and GE in Figure 4.

Some limitations should be considered in this study. (1) VEEG has the potential for false lateralization. However, included cases had unequivocally lateralized VEEG to avoid ambiguity of class labels. (2) Our population had advanced pharmacoresistant TLE, which may not be representative of TLE in general. However, it is typical of an epilepsy surgery population where CADFIG would be most useful. (3) Subgroup analysis is needed to

Author Manuscript Author Manuscript Author Manuscript Author Manuscript

determine reliability of CADFIG in TLE subtypes such as mesial temporal sclerosis and cortical dysplasia. (4) Although our sample size was large enough to permit reasonable assessment of overall predictive accuracy in lateralized TLE, the non-concordant MRI subgroup size was only moderate. Validation with larger samples and multi-site data are needed to completely assess the utility of CADFIG. (5) Due to moderate sample size, cross-validation was used to estimate classification performance. External test validation is needed to fully evaluate classification performance. Cross-validation estimates may possibly be biased upward from performance attained from external testing. However, even more conservative methods of double cross-validation still attained high performance accuracy (90.0%, right TLE; 85.7%, left TLE; 87.5%, overall). (6) To compare with the current standard of care, CADFIG was compared to qualitative expert MA of MRI. Research using quantitative MRI is also needed for comparison. (7) Due to a limited number of bilateral TLE patients in our study sample, this population was not considered. Patients with major neurological/psychiatric co-morbidities were also excluded to avoid network abnormalities from other conditions. These TLE subgroups represent extensions which should be considered in future work, requiring larger sample sizes to learn noisier statistical patterns. (8) Validation in other focal epilepsies is also necessary prior to use in clinical practice.

In conclusion, we demonstrated that fMRI can potentially be used to identify the affected hemisphere in TLE during the pre-surgical epilepsy assessment, using fMRI features based on functional topology. We showed that fMRI-based tests, such as CADFIG, can discriminate left and right TLE with high sensitivity, both when standard MRI sequences are normal and abnormal. In cases with non-lateralizing MRI sequences, CADFIG predicted the affected hemisphere with high sensitivity. When lateralizing abnormalities were visible on MRI, CADFIG showed high agreement with MA. Used together, a combination of MA and fMRI correctly predicted epileptogenic focus laterality for all cases. With further validation from larger samples and multi-center data, fMRI-based tests such as CADFIG, which exploit differences in functional topology, can improve epileptogenic zone identification in TLE.

Supplementary Material

Refer to Web version on PubMed Central for supplementary material.

Acknowledgments

The authors thank Raja Muthupillai for help with optimizing imaging protocols, and Claudio Arena, Cynthia Calija, and Blanca Vanessa Yataco Marquez for assistance in study participant recruitment.

Grant Support:

Contract grant sponsor: Epilepsy Foundation of America (Research Grants Program); Contract grant sponsor: Baylor College of Medicine Computational and Integrative Biomedical Research Center (CIBR) Seed Grant Awards; Contract grant sponsor: ARCO Foundation Young Teacher-Investigator Award and the Naman Family Fund for Basic Research from the Baylor College of Medicine; Contract grant sponsor: National Library of Medicine Training Fellowship in Biomedical Informatics, Gulf Coast Consortia for Quantitative Biomedical Sciences; Contract grant number: 2T15LM007093-21; Contract grant sponsor: National Institute of Health; Contract grant number: 5T32CA096520-07; Contract grant sponsor: The Moody Foundation.

Author Manuscript Author Manuscript Author Manuscript Author Manuscript

References

1. Berg AT, Vickrey BG, Langfitt JT, et al. The multicenter study of epilepsy surgery: recruitment and selection for surgery. Epilepsia. 2003; 44:1425–1433. [PubMed: 14636351]
2. Haneef Z, Chen DK. Functional neuro-imaging as a pre-surgical tool in epilepsy. Ann Indian Acad Neurol. 2014; 17:S56–64. [PubMed: 24791091]
3. Rosenow F, Luders H. Presurgical evaluation of epilepsy. Brain. 2001; 124:1683–1700. [PubMed: 11522572]
4. Keihaninejad S, Heckemann RA, Gousias IS, et al. Classification and lateralization of temporal lobe epilepsies with and without hippocampal atrophy based on whole-brain automatic MRI segmentation. PLoS One. 2012; 7:e33096. [PubMed: 22523539]
5. Lopes R, Steinling M, Szurhaj W, Maouche S, Dubois P, Betrouni N. Fractal features for localization of temporal lobe epileptic foci using SPECT imaging. Comput Biol Med. 2010; 40:469–477. [PubMed: 20346449]
6. Bullmore ET, Bassett DS. Brain graphs: graphical models of the human brain connectome. Annu Rev Clin Psychol. 2011; 7:113–140. [PubMed: 21128784]
7. Doelken MT, Richter G, Stefan H, et al. Multimodal coregistration in patients with temporal lobe epilepsy--results of different imaging modalities in lateralization of the affected hemisphere in MR imaging positive and negative subgroups. AJNR Am J Neuroradiol. 2007; 28:449–454. [PubMed: 17353311]
8. Fox MD, Snyder AZ, Vincent JL, Corbetta M, Van Essen DC, Raichle ME. The human brain is intrinsically organized into dynamic, anticorrelated functional networks. Proc Natl Acad Sci U S A. 2005; 102:9673–9678. [PubMed: 15976020]
9. Liang X, Wang J, Yan C, et al. Effects of different correlation metrics and preprocessing factors on small-world brain functional networks: a resting-state functional MRI study. PLoS One. 2012; 7:e32766. [PubMed: 22412922]
10. Power JD, Barnes KA, Snyder AZ, Schlaggar BL, Petersen SE. Spurious but systematic correlations in functional connectivity MRI networks arise from subject motion. Neuroimage. 2012; 59:2142–2154. [PubMed: 22019881]
11. Tzourio-Mazoyer N, Landeau B, Papathanassiou D, et al. Automated anatomical labeling of activations in SPM using a macroscopic anatomical parcellation of the MNI MRI single-subject brain. Neuroimage. 2002; 15:273–289. [PubMed: 11771995]
12. Wang JH, Zuo XN, Gohel S, Milham MP, Biswal BB, He Y. Graph theoretical analysis of functional brain networks: test-retest evaluation on short- and long-term resting-state functional MRI data. PLoS One. 2011; 6:e21976. [PubMed: 21818285]
13. Chiang S, Haneef Z. Graph theory findings in the pathophysiology of temporal lobe epilepsy. Clin Neurophysiol. 2014; 125:1295–1305. [PubMed: 24831083]
14. Haneef Z, Lenartowicz A, Yeh HJ, Engel J Jr, Stern JM. Effect of lateralized temporal lobe epilepsy on the default mode network. Epilepsy Behav. 2012; 25:350–357. [PubMed: 23103309]
15. Bettus G, Bartolomei F, Confort-Gouny S, et al. Role of resting state functional connectivity MRI in presurgical investigation of mesial temporal lobe epilepsy. J Neurol Neurosurg Psychiatry. 2010; 81:1147–1154. [PubMed: 20547611]
16. Wilke C, Worrell G, He B. Graph analysis of epileptogenic networks in human partial epilepsy. Epilepsia. 2011; 52:84–93. [PubMed: 21126244]
17. Powell HW, Richardson MP, Symms MR, et al. Reorganization of verbal and nonverbal memory in temporal lobe epilepsy due to unilateral hippocampal sclerosis. Epilepsia. 2007; 48:1512–1525. [PubMed: 17430404]
18. Liu M, Chen Z, Beaulieu C, Gross DW. Disrupted anatomic white matter network in left mesial temporal lobe epilepsy. Epilepsia. 2014; 55:674–682. [PubMed: 24650167]
19. Doucet GE, Skidmore C, Sharan AD, Sperling MR, Tracy JI. Functional connectivity abnormalities vary by amygdala subdivision and are associated with psychiatric symptoms in unilateral temporal epilepsy. Brain Cogn. 2013; 83:171–182. [PubMed: 24036129]
20. Lynall ME, Bassett DS, Kerwin R, et al. Functional connectivity and brain networks in schizophrenia. J Neurosci. 2010; 30:9477–9487. [PubMed: 20631176]

Author Manuscript Author Manuscript Author Manuscript Author Manuscript

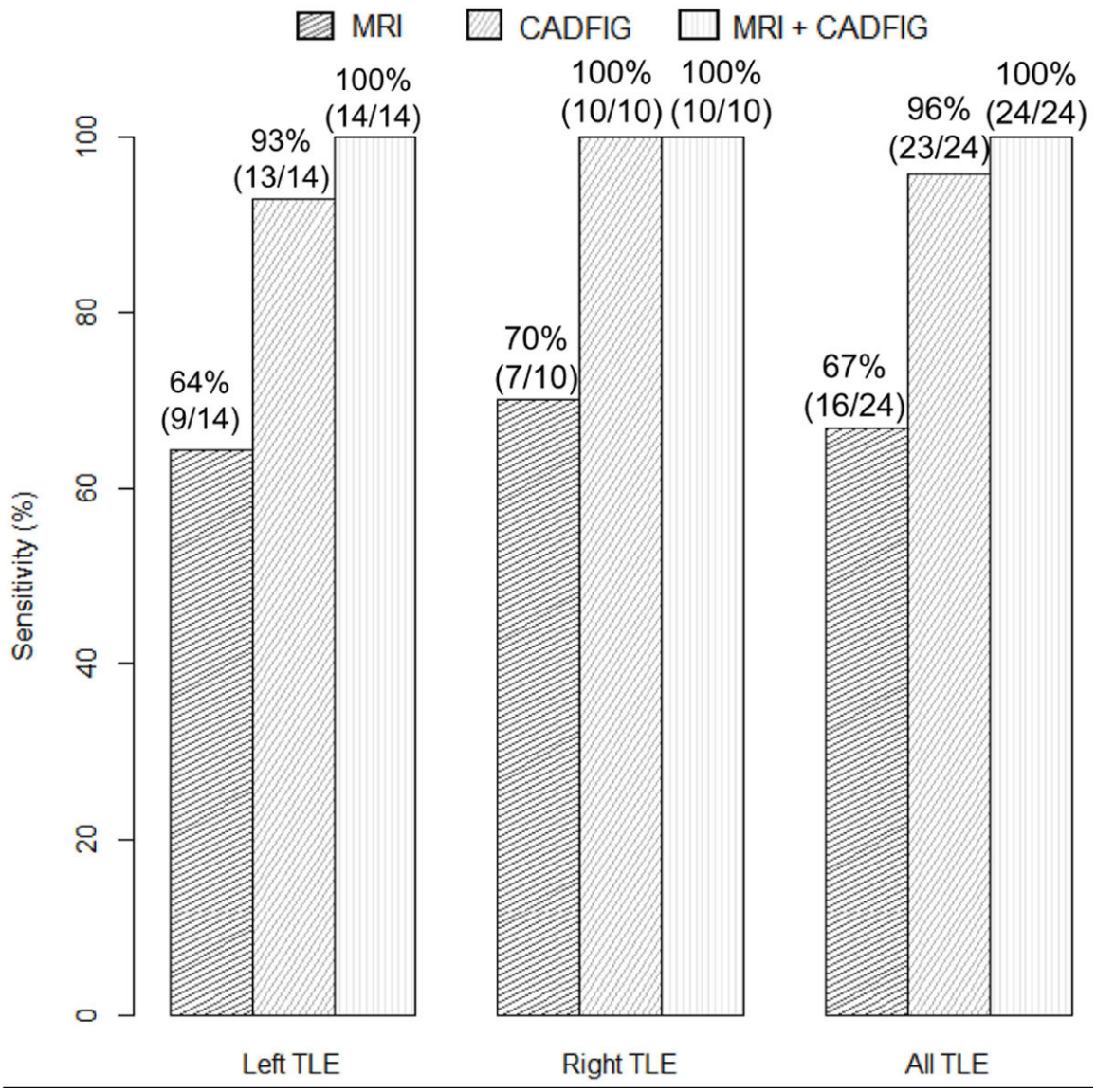

Figure 1.

Sensitivity of manual analysis of high-resolution structural MRI (MA), CADFIG, and combined approach of MA and CADFIG in lateralizing left and right TLE. Proportion of correctly lateralized patients are shown above the corresponding bars. TLE, temporal lobe epilepsy.

Author Manuscript Author Manuscript Author Manuscript Author Manuscript

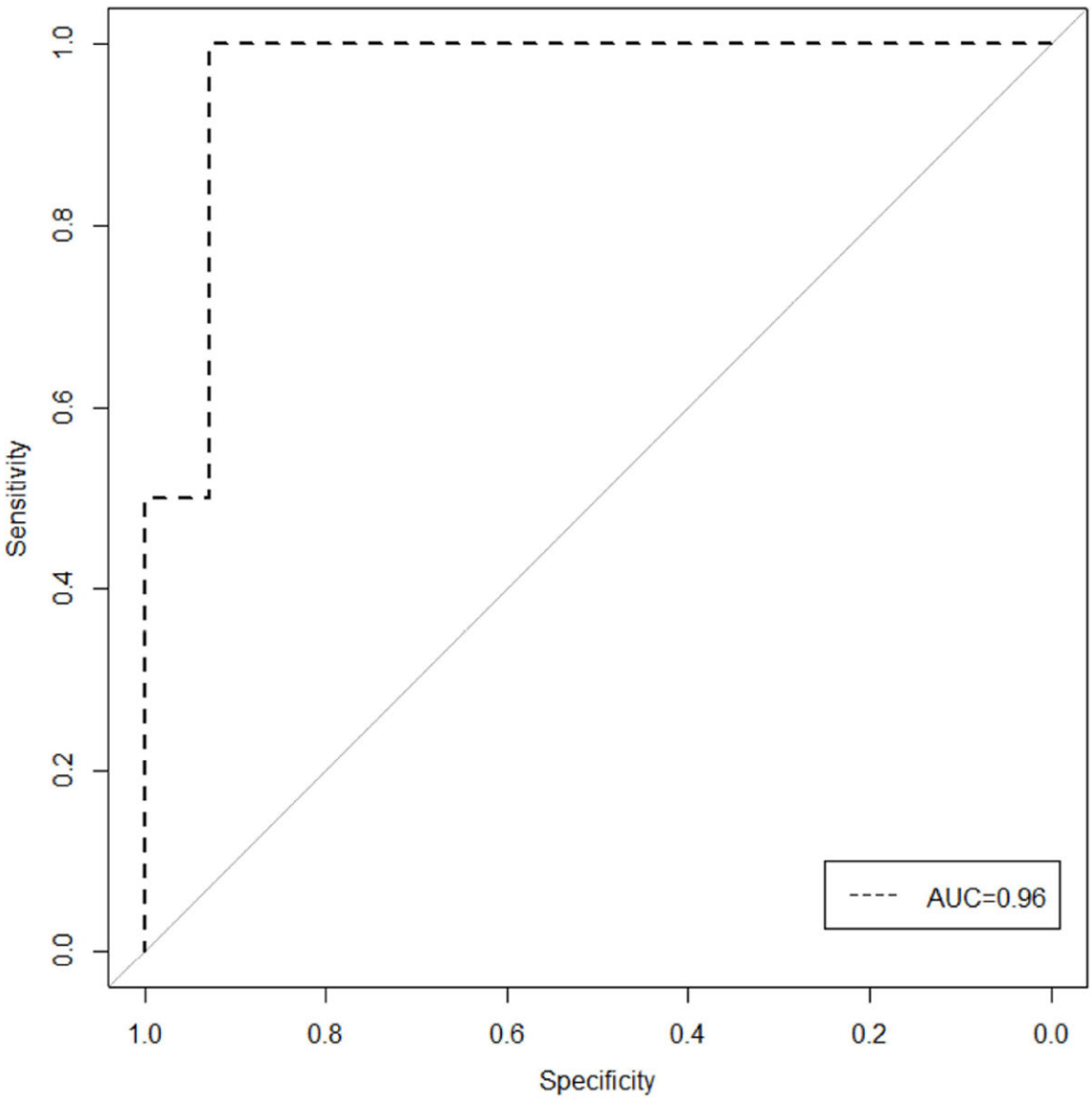

Figure 2.
Receiver operating characteristic (ROC) curve for classification performance of CADFIG. AUC, area under the ROC curve.

Author Manuscript Author Manuscript Author Manuscript Author Manuscript

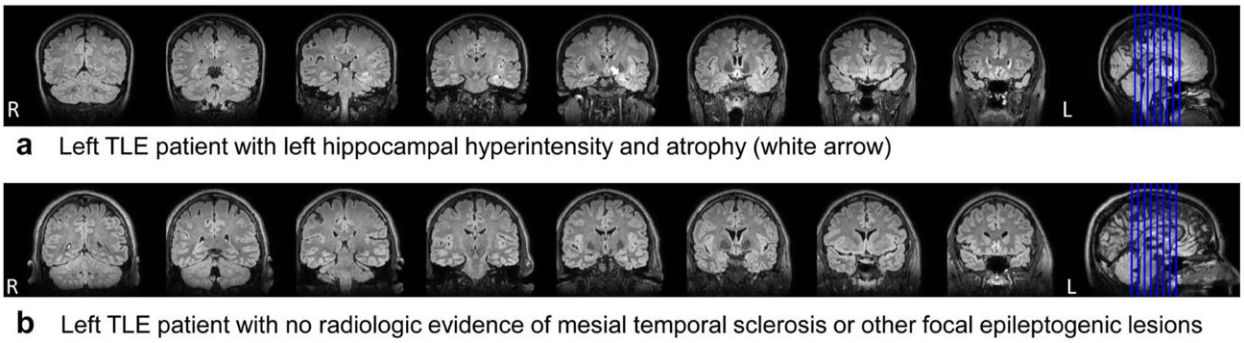

Figure 3.

FLAIR images from (a) a left TLE patient with left hippocampal hyperintensity and atrophy (white arrow) in keeping with mesial temporal sclerosis (Subject 1), and (b) a left TLE patient with non-lateralizing MRI (Subject 13). For the subject shown in (a), both MA and CADFIG correctly identified the affected hemisphere. For the subject shown in (b), MRI sequences were non-lateralizing but CADFIG was able to accurately identify focus laterality. Images are displayed in radiologic convention.

Author Manuscript Author Manuscript Author Manuscript Author Manuscript

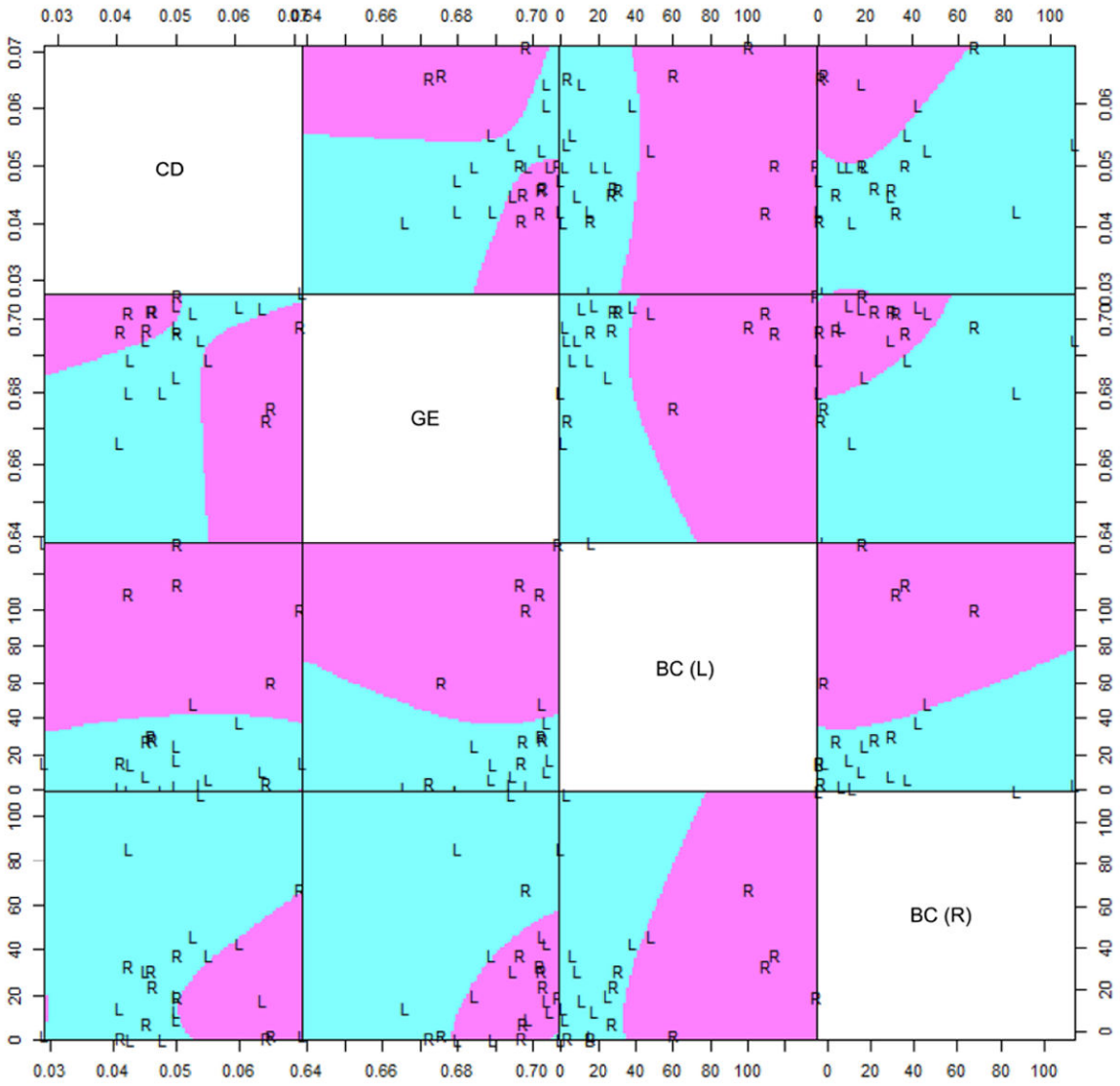

Figure 4.

Scatterplot matrix visualizing separation of left (L) and right (R) TLE subjects based on variables identified from optimal feature subset (connectivity diversity, global efficiency, and betweenness centrality of the left and right hippocampi). Purple and turquoise areas indicate whether future out-of-sample observations would be classified as right (purple) or left (turquoise) TLE, based on a quadratic discriminant function trained on the sample examined in this study. *x*- and *y*-axes are given by the corresponding graph theory metrics listed on the main diagonal. CD, connectivity diversity; GE, global efficiency; BC (L), left hippocampal betweenness centrality; BC (R), right hippocampal betweenness centrality.

Author Manuscript

Author Manuscript

Author Manuscript

Author Manuscript

Table 1

Discriminatory power of fMRI graph theory measures when considered in univariate and multivariate discriminatory contexts. Univariate discriminatory power was assessed based on the Fisher separability criterion (FSC). Multivariate discriminatory power was assessed using a backward stepwise variable importance measure (BSVI), calculated based on the increase in LOO-CV error with removal of the variable from the optimal feature set.

	Univariate (FSC)	Multivariate (BSVI)
CD	0.125	0.292
CS	0.329	--
γ	0.124	--
λ	0.216	--
σ	0.023	--
GE	0.220	0.333
BC (L)	1.468	0.292
BC (R)	0.089	0.125
CC (L)	0.099	--
CC (R)	0.177	--
LE (L)	0.007	--
LE (R)	0.064	--

Abbreviations: BC (L), left hippocampal betweenness centrality; BC (R), right hippocampal betweenness centrality; BSVI, backward stepwise variable importance measure; CC (L), local clustering coefficient of left hippocampus; CC (R), local clustering coefficient of right hippocampus; CD, connectivity diversity; CS, connectivity strength; FSC, Fisher separability criterion; LE (L), local efficiency of left hippocampus; LE (R), local efficiency of right hippocampus; γ, clustering coefficient; λ, path length; σ, small-world index